12th CIRP Conference on Photonic Technologies [LANE 2022], 4-8 September 2022, Fürth, Germany

Adaptive control for a dual laser beam solution for the welding of high reflectivity dissimilar materials

Beñat Arejita[a,b,*], Juan Fernando Isaza[a], Miguel Antunez[a], Aitzol Zuloaga[b]

a EXOM Engineering, Avenida Altos Hornos de Vizcaya 33, Barakaldo 48901, Spain
b UPV/EHU, Ingeniero Torres Quevedo Plaza 1, Bilbao 48013, Spain

* Corresponding author. Tel.: +34-623-108-883. *E-mail address:* benat.arejita@exomengineering.com

Abstract

The laser welding technology delivers high flexibility and adaptability to the welding process being able to adjust to complex joint geometries. Additionally, the application of a laser beam minimises the microstructural changes in the material due to the low heat application and low thermal distortion that the technology offers. Due to these advantages, laser welding technology is being adopted in technologically demanding markets such as EV battery manufacturing. However, these new application areas present challenges that must be overcome, such as joining dissimilar materials with different melting points and high reflectivity values in the typical laser wavelengths (Al, Cu). This work presents an adaptive control method for joining high reflectivity dissimilar materials using a dual laser beam setup to overcome these problems. As a result, a comparative study of different pulsed and continuous-wave laser arrangements through static and dynamic optics and the obtained joining qualities is presented.

Keywords: Laser Beam Welding; Fast Beam Manipulation; Dissimilar Materials; Dynamic Process Control; Edge Computing

1. Introduction

The laser welding of dissimilar metals is a technique experiencing significant momentum in different industrial applications. On the one hand, structural engineering applications will benefit from the joining of light material with high strength resulting in a reduction in the weight of structures and vehicles. On the other hand, the electrification of vehicles can also take advantage of the laser welding of high conductivity materials such as aluminum and copper. Nevertheless, the laser welding of dissimilar materials presents challenges that must be overcome [1]. For instance, the difference in physical properties of the materials, such as the melting temperature, can complicate the joining process. Moreover, materials such as aluminum and copper present very low absorptivity in the IR range and have a high thermal conductivity, which hinders the welding process using typical laser beam sources. In order to overcome these challenges, the applied laser energy density must be tailored for each type of material combination so that the formation of intermetallic compounds (IMC) is minimized, thus assuring an optimal bonding that provides the desired electrical and mechanical properties [2]. In the case of high reflectivity materials, the tailored energy distribution can be achieved by oscillating the laser beam (wobbling), where the oscillating frequency, the oscillating amplitude, the oscillating pattern, the laser power, and the welding speed directly influence the weld formation and its quality [3]. Additionally, the usage of the wobbling technique allows for obtaining good joints also when a lower quality laser source is used, as the melt pool is enlarged and evenly distributed with the oscillatory movement [4]. However, the oscillating movement generates local laser beam intensity peaks that depend on the wobbling pattern if a constant laser power is commanded. In order to compensate for these

localized intensity peaks that directly affect the energy distribution on the material, tailored power distributions can be designed to generate uniform intensity profiles for each oscillation [5]. This approach leads to superpositioned spatial and temporal power modulation techniques, where both the laser power modulation and the laser beam wobbling strategy are carefully designed to provide optimal energy densities, obtaining a compensated weld penetration [6]. In addition, the frequency and amplitude of the laser beam oscillation influence the penetration depth, which directly impacts the resistivity of the joint [7]. On the other hand, the usage of diffractive optical elements (DOE) can achieve tailored laser profiles that meet the requirements of the welding process, being able to generate ring profiles, line profiles, or even multiple spot profiles [8]. Both laser oscillation welding and beam shaping are promising techniques that help overcome the challenges of welding high-reflectivity dissimilar materials. Recent studies have shown that novel fiber laser beam shapes with a central laser spot surrounded by a secondary ring shape beam can further improve the stability of the weld [9,10]. Nevertheless, the typical laser beam oscillation systems present maximum oscillation frequencies in the range of 2-4 kHz. For high throughput process requirements such as e-mobility component production, new laser source technologies rely on coherent beam combining (CBC) and optical phase arrays (OPA), generating high power tailored beam profiles at frequencies up to 1 MHz [11].

In this work, we present a compact industrial dual laser beam welding head that can be used to generate complex welding strategies that result in custom energy distributions tailored to weld high reflectivity dissimilar materials. We also present preliminary test results of the lap joint welding of copper (Cu-EPT, CW004A) to aluminum (AlMgSi0,5) using different welding strategies from mono beam modes to dual-beam modes with adaptive power control.

Nomenclature

Q	laser spot power [W]
r_0	radius of the focused spot [mm]
η	laser energy attenuation factor
v	welding speed [mm/s]
(x_0, y_0)	initial position of the laser spot [mm]
f	wobbling frequency [Hz]
(A, B)	wobbling amplitudes in the x and y direction [mm]
(dc, T)	duty cycle [%] and period [s] of the pulsed laser

2. Dual Laser welding head and optical setup

The research work presented in this paper has been implemented with the SO3 industrial version of the dual laser beam optical scanning head, which consists of four basic modules and the SdLED control card depicted in Fig. 1.

The core of the optical head is represented by the Scanner Module (Fig. 1-1), which deflects a collimated laser beam with an aperture of 20 mm through the movement of two mirrors, each one mounted on a galvanometer motor. The aluminum body is actively cooled by water and embeds the control card. It exposes the interface ports to integrate connection signals

with the PLC and the HMI and communicate with the sensors and cameras.

The Beam Bender Module (Fig. 1-2) mounts a dichroic mirror deflecting the incoming laser radiation at 630/1070 nm by 90° and allowing visible light (VIS at 400-700 nm) and infrared radiation to pass through (IR 1100-3500 nm). The beam bender module is designed to be installed at the scanner entrance or as an extra module on top of the scanner body to combine two independent laser beams, which is the configuration presented in this work. Thus, the solution can combine a VIS camera with SWIR/MWIR cameras for process monitoring and control with different fiber laser beams.
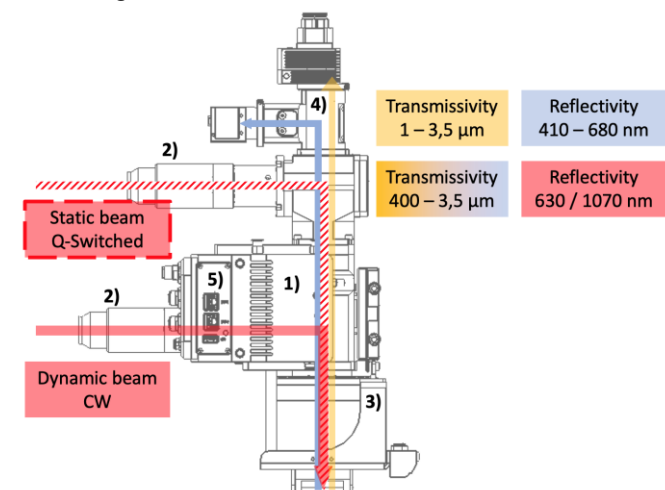

Fig. 1. Dual laser welding head optical setup. 1) Scanner module, 2) Beam bender module, 3) Focusing module, 4) Camera module, 5) SdLED control card.

The focusing module (Fig. 1-3) incorporates a large aperture lens holder to insert a flat 3-inch focusing lens and a protection window. Lenses with different focal lengths can be installed in the cassette. For the tests carried out during the experimentation, a 250 mm focal length was used. Additionally, an illumination light has been added to improve the exposure intensity of the VIS camera images, preparing the optics for machine vision solutions supervising the welding process. Finally, the focusing module integrates an air curtain to protect the optics from splashes and fumes resulting from the welding process. In order to monitor the process, the camera module (Fig. 1-4) allows a coaxial acquisition of images with respect to the laser beam over the parts to be processed. The process monitoring is done using a visual camera (e.g., IDS GV-5040CP; Global-Shutter CMOS sensor; resolution of 1456 x 1088 pixels at 3.45 µm pixel size; up to 78.0 fps) and an IR Camera (e.g., Tachyon 1024, MWIR 1 – 5 µm; 32x32 pixels; up to 1000 fps) allowing closed-loop strategies to control the process.

The final principal component is the SdLED® Control Card (Fig. 1-5), which is used to control (among other functionalities) the movement of the galvanometers using the data acquired by the IR camera, being the central processing unit of all peripherals integrated into the system. In this way, the control unit can adapt the intensity of the laser beam and the oscillation strategy of the welding wobble in real-time, and it enables the autonomous operation of the welding head during

material processing, only needing communication with an external PC for the strategy preparation, observation, and quality control of the welding process.

The lasers used for the experimentation part of this work for welding copper (Cu-EPT, CW004A) and aluminum (AlMgSi0,5) in a lap joint were, on the one hand, a single-mode fiber laser (MaxPhotonics) with an output power of 1 kW and a wavelength of 1070 nm, with an optical fiber diameter of 50 µm and a collimator lens with f=100 mm. This laser was coupled with the scanning module resulting in a dynamic beam. On the other hand, a multi-mode fiber laser with an average power of 600 W (IPG-Photonics) and a wavelength of 1070 nm, with a diameter of 50 µm optical fiber and a motorized collimator lens with f=100 mm was used. This second laser source can be pulsed using the q-switching technique, reaching maximum power peaks of up to 6 kW, and in the presented set-up, it was used as a static beam.

3. Tailored energy distributions

The capabilities of the presented dual laser beam welding head allow composing tailored energy configurations by super positioning both laser sources. While the pulsed laser is used to generate the needed material penetration of the welding keyhole, the continuous wave laser beam can be wobbled around the static pulsed beam to spread and stabilize the melt pool. The resulting energy distribution can be modeled as Chen et al. described [3]. Thus, considering a gaussian distribution laser spot, the corresponding energy distribution can be characterized as defined in Eq. 1:

$$q_C(x,y,t) = (1-\eta) \cdot \frac{2Q}{\pi r_o^2} exp\left(-\frac{2[(x-x_L(t))^2+(y-y_L(t))^2]}{r_o^2}\right) \quad (1)$$

In the case of a pulsed laser, the above equation could be reshaped into the following equation for a pulse period:

$$q_p(x,y,t) = \begin{cases} q_C(x,y,t) & if\ 0 < t \le dc \cdot T \\ 0 & if\ dc \cdot T < t \le T \end{cases} \quad (2)$$

The resulting fluence E_T [J/mm²] for a specified period of time can be modeled as defined in Eq. 3:

$$E_T(x,y) = \int_0^T q_C(x,y,t)dt + \int_0^T q_P(x,y,t)dt \quad (3)$$

The movement of both laser spots can be described using Eq. 4, taking into account that the wobbling is done in a clockwise manner and the welding is done in the x direction. The movement of the pulsed spot can be modeled with the same equation considering the cosine and sine amplitudes are equal to 0.

$$\begin{aligned} x_L(t) &= x_0 + vt + 0.5A cos(2\pi f t) \\ y_L(t) &= y_0 + 0.5B sin(2\pi f t) \end{aligned} \quad (4)$$

The usage of different amplitude values A and B in Eq. 4 allows the definition of both circular and elliptical wobbling strategies in a parameterized manner.

When the values of A and B are equal, circular wobbling patterns are generated. Fig. 2 shows a simulation of 0.1 seconds of the resulting energy distribution of a stationary pulsed laser source and a concentric circular wobble using a continuous wave laser.
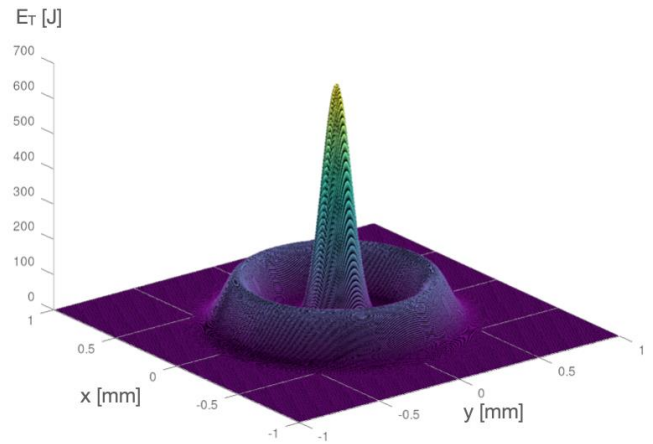

Fig. 2. Simulated resulting fluence with circular wobbling. Pulsed laser configuration; power: 3000 W, frequency: 100 Hz and duty cycle: 10%. Continuous wave scanned laser configuration; power: 1000 W, A: 1 mm, B: 1 mm, wobble frequency: 1000 Hz. Welding scan velocity of 0 mm/s, r_0: 0.15 mm and a laser energy attenuation factor of 0.2.

On the contrary, when the values of A and B are different, elliptical wobbling patterns are generated. As the frequencies of both sine and cos functions are the same but the amplitudes are not equal, there is a concentration of points in the vertices of the ellipse, resulting in a higher energy deposition near those areas. Fig. 3 shows a simulation of 0.1 seconds of the resulting energy distribution of the combination of a stationary pulsed laser source and a concentric elliptical wobble using a continuous wave laser.
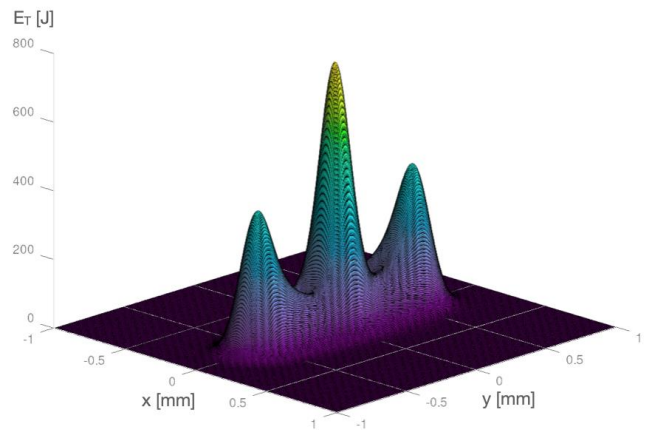

Fig. 3. Simulated resulting fluence with elliptical wobbling. Pulsed laser configuration; power: 3000 W, frequency: 100 Hz and duty cycle: 10%. Continuous wave scanned laser configuration; power: 1000 W, A: 0.2 mm, B: 1.2 mm, wobble frequency: 1000 Hz. Welding scan velocity of 0 mm/s, r_0: 0.15 mm and a laser energy attenuation factor of 0.2.

The dual laser setup can then be used in different welding scenarios by mounting the welding head on an industrial robot, a gantry system, or by moving the workpiece in relation to the scanner head. Eq. 4 takes into consideration welding

movements in the x-direction. Nevertheless, the formula can be modified to include the y velocity factor. Fig. 4 shows a simulation of 0.1 seconds of the resulting energy distribution of the combination of a pulsed laser source and a concentric circular wobble using a continuous wave laser with a welding movement in the x-direction.
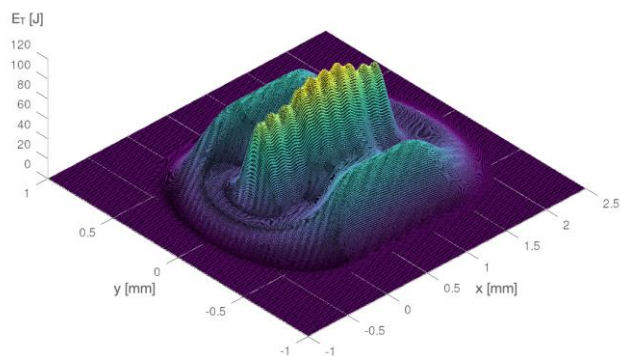

Fig. 4. Simulated resulting fluence with circular wobbling and welding scan in the x direction. Pulsed laser configuration; power: 3000 W, frequency: 100 Hz and duty cycle: 10%. Continuous wave scanned laser configuration; power: 1000 W, A: 0.2 mm, B: 1.2 mm, wobble frequency: 1000 Hz. Welding scan velocity of 16.6 mm/s advancing 1.66 mm in the simulation time of 0.1 seconds, r_0: 0.15 mm and a laser energy attenuation factor of 0.2.

4. Results

The presented technology offers an infinite number of possibilities when it comes to generating wobbles using the dual-laser beam configuration since each wobble can be made up of n trajectories, each with its own speed and power, combined with the pulsed laser in the multiple configurations of pulse width, duty cycle, laser power, and focal plane. Different wobble strategies have been tested as initial experimentation and demonstration tests of the multi-beam welding laser head. All the welding strategies implemented in this experimentation phase used an elliptical wobble for the CW laser (A) combined with the resulting spot from the pulsed laser (B). The parameter ranges used during the tests are presented in Table 1.

Table 1. Parameter ranges used during the tests.

Setup Parameter	Laser A	Laser B
Power [Watt]	600 - 1000	2750 – 3600
Pulse frequency [Hz]	NA	100 - 500
Duty Cycle [%]	NA	4 - 20
Ellipse width and height	0.1 – 0.6	NA
Wobble Frequency [Hz]	500 - 2064	NA
Feed Speed [m/min]	0.25 – 1.5	0.25 – 1.5

Some examples of these initial results obtained for Cu/Al welding are described below and shown in Fig. 2.

4.1. Mono mode with dynamic beam (a)

In this configuration, laser A was switched on, emitting a continuous power of 1000 W, and the wobbling strategy was elliptical with a wobbling frequency of 1608 Hz and size 0.2x0.6 (WxH). Laser B was switched off, resulting in a typical mono beam wobbling configuration. This configuration was not able to affect the copper, and its results are not depicted in Fig. 1.

4.2. Mono mode with static pulsed beam (b)

Laser A was switched off for this test, resulting in a static beam configuration, while laser B was pulsing at 3250 W with a pulse-on time of 0.4 ms and a pulse frequency of 100 Hz. As shown in Fig. 2-b, the pulses resulted in a very narrow seam with an average seam width of 287 μm.

4.3. Dual mode without adaptive control (c, d)

In the case of the dual-mode configuration, both lasers A and B were emitting. In this configuration, different tests were carried out. The first test had the following settings: laser A was configured to 1000 W, and laser B emitted at a peak power of 3000 W. The same wobbling strategy as test a was used for the dynamic beam. This test showed that the melt pool tended to be unstable along the path with an average width of 372 μm, as depicted in Fig. 2-c. In order to improve the results, the following modifications were made to improve the resulting seam by increasing the power of the pulsed laser to 3250 W, obtaining a more substantial piercing effect on the pulsed laser to material interaction. As shown in Fig. 2-d, the resulting seam did present some improvements resulting in an average seam width of 425 μm.

4.4. Dual mode without adaptive control and surface pre-heating (e)

Under this test, the surface of the copper sheet was preheated to explore possible improvements in the stability of the welding process. The area to be processes was preheated by several wobbling passes with low power configurations that did not result in melting temperatures of the material. The system configuration was the same as the one described in test d. The resulting seam showed a better weld in the test specimen (avg. width 468 μm), possibly due to the stabilization of the material's preheating, as can be observed in Fig. 2-e.

4.5. Dual mode with adaptive control (f)

In the previous cases, it was clear that it was difficult to stabilize the melt pool without controlling the temperature distribution on the surface. This resulted in poor seams even though the copper was successfully welded to the aluminum. In order to control the temperature of the process, a closed-loop power control was used using a PID. The controller dynamically adapted the power of the CW laser using the frames of the IR as the input to the controller with a control cycle time of 1 ms. The wobbling strategy was the same as in

the other tests, and the pulsed laser was set with the same parameters as in test e. These settings resulted in the most promising configuration, as the process was able to weld the copper to aluminum satisfactorily with the best seam quality (avg. width 579 μm) in comparison to the rest of the tests carried out during the experimentation, as shown in Fig. 2-f.
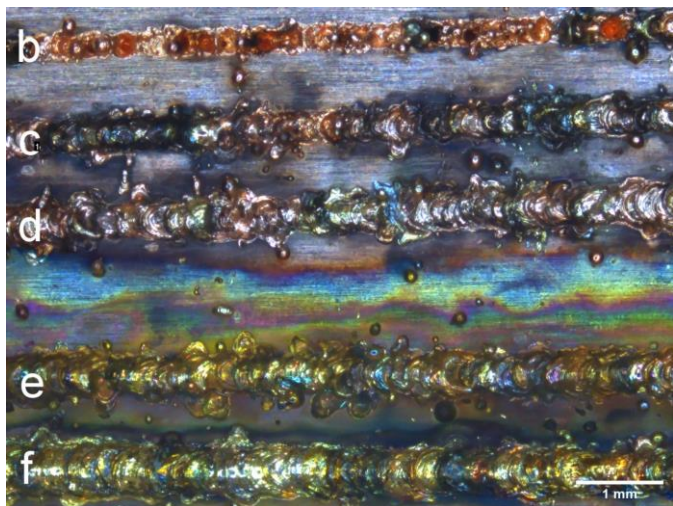

Fig. 5. Test results: b) mono mode with static pulsed beam, c) dual mode without adaptive control (pulsed power 3 kW), d) dual mode without adaptive control (pulsed power 3.25 kW), e) Dual mode without adaptive control and surface pre-heating, f) Dual mode with adaptive control.

5. Conclusion

A dual laser beam solution integrating cameras in the visual and infrared range has been presented. The combination of two laser beams emitting in the same wavelength but operating in different modes, together with scanning optics enables a defined energy distribution for dissimilar material welding in lap joint. This weld takes advantage of the concentrated energy input of the pulsed modus in combination with the high spatial modulation of the CW laser widening the melt pool and stabilizing the resulting seam. The integration in the optics of a closed loop control benefits the stability of the weld independently of the length and width of the welded sheets, but also enables a near side-by-side positioning of the seams increasing the contact surface of the materials, without increasing the cooling down time between every weld.

References

[1] Kurynstsev S. A review: laser welding of dissimilar materials (Al/Fe, Al/Ti, Al/Cu)—Methods and techniques, microstructure and properties. Materials 2022; 15-122.
[2] Indhu R, Soundarapandian S, Vijayaraghavan I. Yb: YAG laser welding of dual phase steel to aluminium alloy. Joournal of Materials Processing Tech 2018; 262, p. 411-421.
[3] Chen L, Wang C, Mi G, Zhang X. Effects of laser oscillating frequency on energy ditribution, molten pool morphology and grain structure of AA6061/AA5182 aluminum alloys lap welding. Journal of Materials Research and Technology 2021; 15, p. 3133-3148.
[4] Fortunato A, Ascari A. Laser welding of thin copper and aluminum sheets: feasability and challenges in continuous-wave welding of dissimilar metals. Lasers in Manufacturing and Materials Processing 2019, 6, p. 137-157.
[5] Kraetzsh M, Standfuss J, Klotzbach A, Kaspar J, Brenner B, Beyer E. Laser beam welding with high-frequency beam oscillation: welding of dissimilar materials with brilliant fiber lasers. Physics Procesia 2011; 12, p. 142-149.
[6] Hummel M, Häusler A, Gillner A. High-precission adjustment of welding depth during laser micro welding of copper using superpositioned spatial and temporal power modulation. J. Manuf. Mater. Process. 2021; 5-127.
[7] Jarwitz M, Fetzer F, Weber R, Graf T. Weld seam geometry and electrical resistance of laser-welded, aluminum-copper dissimilar joints produced with spacial beam oscillation. Metals 2018, 8-510.
[8] Rasch M, Roider C, Kohl S, Strauss J, Maurer N, Nagulin KY, Schmidt M. Shaped laser beam profiles for heat conduction welding of aluminium-copper alloys. Optics and Lasers in Engineering 2019; 115, p. 179-189.
[9] Wang L, Mohammadpour M, Gao X, Lavoie JP, Kleine K, Kong F, Kovacevic R. Adjustable Ring Mode (ARM) laser welding of stainless steels. Optics and Lasers in Engineering 2021; 137-106360.
[10] Maina MR, Okamoto Y, Okada A, Närhi M, Kangastupa J, Vihinen J. High surface quality welding of aluminum using adjustable ring-mode fiber laser. Journal of Materials Processing Tech. 2018; 258, p. 180-188.
[11] Prieto C, Vaanomnde E, Diego-Vallejo D, Jimenez J, Urbach B, Vidne Y, Shekel E. Dynamic laser beam shaping for laser aluminium welding in e-mobility applications. Procedia CIRP 2020; 94, p. 596-600.